GPS-INS Integration for Autonomous Navigation of Aircrafts

Saurav Agarwal[1], Vaibhav V Unhelkar[2],
Avnish Kumar[4], Hari B Hablani[5]
Department of Aerospace Engineering
Indian Institute of Technology Bombay
Mumbai, India

Anuj Sharma[3]

Department of Aerospace Engineering
Indian Institute of Technology Kanpur
Kanpur, India

***Abstract*—The advent of Global Navigation Satellite Systems has brought about an additional navigational aid for aircrafts. Due to their complementary error characteristic, various approaches involving Global Positioning System coupled with the Inertial Navigation System have been looked into for complete autonomous navigation and attitude estimation of the aircraft. In this paper, we study, through simulation, approaches of GPS-INS integration based on the extended Kalman filter. An open-loop tightly-coupled GPS-INS integration approach utilizing raw pseudorange measurements is analyzed in presence of realistic measurement errors. Improvements in the approach, via bias estimation and carrier phase tracking have also been briefly examined. Lastly, a computationally efficient approach to resolve integer ambiguities for carrier phase tracking is also simulated. Although the results presented are based on GPS simulation, the analysis is equally applicable to other satellite navigation systems due to their similar operating principles.**

Keywords—Extended Kalman Filter, GPS-INS integration

I. INTRODUCTION

Global Navigation Satellite Systems are increasingly becoming more and more important for cost-effective navigation of aircrafts. Apart from the global navigation systems, a regional navigation satellite system for India, named the Indian Regional Navigational Satellite System (IRNSS), is being developed by the Indian Space Research Organization (ISRO). The presence of Global Positioning System (GPS) receivers has become commonplace in today's world, and various aircrafts ranging from commercial jets to micro aerial vehicles are equipped with GPS receivers, albeit of different accuracies.

Inertial Navigation System (INS), a dead-reckoning navigational aid, includes the sensors – accelerometers and gyros – for measurement of linear acceleration and angular rates, respectively. These measurements are available at a very high rate (~100 Hz) and are suitably integrated to obtain the aircraft's position, velocity and attitude (orientation) [1]. However, the measurements from these sensors are erroneous due to the presence of random errors and unknown biases. Moreover, these errors increase with time, and, thus, need to be periodically corrected for using some external aid.

GPS receivers, which are used to obtain the position and velocity of the aircrafts, on the other hand, do not provide measurements as frequently as the INS. However, the errors exhibited by the GPS do not grow with time. Due to this complementary error characteristic of GPS and INS, various approaches involving GPS coupled with the INS have been investigated by researchers for complete navigation and attitude estimation of the aircraft [2-4].

In this paper, we study, through simulation, approaches of GPS-INS integration which utilize the Kalman filter framework. We first analyze an open-loop tightly-coupled GPS-INS integration approach, which utilizes raw measurements from a stand-alone single-frequency GPS receiver. Due to inherent limitations in accuracy that arise due to a single-frequency GPS receiver, improvements are required for critical aircraft applications. Hence, techniques for improved accuracy of GPS measurements, namely, differential-GPS (DGPS) and carrier phase are simulated. However, carrier phase, although significantly accurate is also equally challenging, specifically due to the need to resolve integer ambiguities. So, a computationally efficient approach to resolve integer ambiguities is presented. The paper concludes with simulation results of aircraft landing, with aiding from carrier phase GPS measurements. Although, the work here includes results based on GPS simulation, the analysis presented is applicable to other satellite navigation systems (both regional and global) as well due to their similar operating principles.

II. MOTIVATION

To better demonstrate the need for GPS-INS integration, we first simulate and observe the performance of aircraft navigation systems without any INS aiding. An aircraft flight is simulated from Srinagar to Kanyakumari, for which the navigation is done through an unaided INS [5]. No biases are considered for the accelerometer and gyro measurements, and the measurement error has been modeled as white noise. The values for the gyro and accelerometer white noise power spectral densities (PSD) are taken as, 4.84×10^{-7} $(\text{deg/s})^2/\text{Hz}$ and 2.26×10^{-7} $(\text{m/s}^2)^2/\text{Hz}$, respectively, and are assumed to be identical for all the three axes.

[1] *Research Assistant*, email: saurav6@gmail.com
[2] *M. Tech Student*, email: v.unhelkar@iitb.ac.in
[3] *B. Tech Student*, email: anuj1819@gmail.com
[4] *B. Tech Student*, email: avnish_10_chd@iitb.ac.in
[5] *Professor*, email: hbhablani@aero.iitb.ac.in

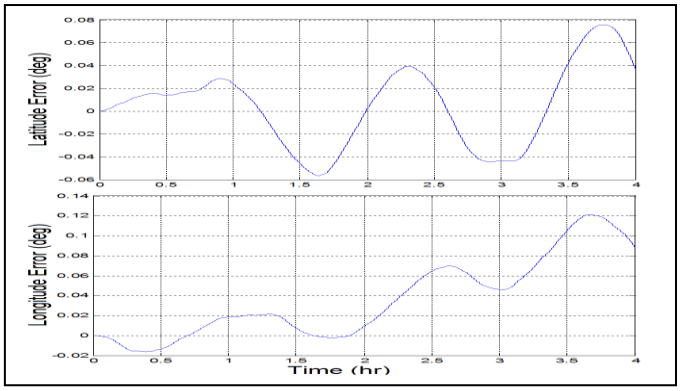

Figure 1. Latitude-Longitude Error: INS only navigation

In spite of assuming low noise and no bias in the measurement, limitations of an unaided INS are evident from Fig. 1, which shows the errors in aircraft latitude and longitude. The resulting error in position increases to around 10 km at the end of the flight trajectory. Similar unacceptable errors are observed in aircraft's attitude and velocity [5]. Further, precise navigation with a GPS only system is also not viable both due to the available positioning accuracy and its inherent low rate. Having understood the motivation of integrating GPS and INS measurements, the following section briefly describes GPS-INS integration approaches which provide a pragmatic navigation system.

III. GPS-INS Integration Approaches

Several GPS-INS integration approaches, differing in their complexity and accuracy, exist in the literature. The crudest from is to obtain a solution of position and velocity estimates from GPS measurements, and use them to reinitialize the INS. In this case the equations of GPS and INS are totally uncoupled. The variation in integration architectures lies in mainly three fields,

- Method of INS error correction by GPS measurements,
- Type of GPS measurement being used, and
- Way in which GPS receiver is aided by the INS.

In all the approaches of GPS-INS integration, Kalman filter (or its variations) is used, due to its optimality and capability for multi-sensor fusion. Based on the above parameters the various GPS-INS approaches are broadly classified as, *Loosely*, *Tightly*, and *Deeply* coupled [4]. Additionally, depending upon whether the correction is applied to reinitialize the INS after every time-step, or not, we have open and close loop architectures. The approach presented in the next section is open-loop tightly coupled architecture since the navigation corrections are not used to reset the INS propagation equations, and raw pseudorange measurements are used to aid the INS.

IV. Modeling and Formulation

In this section, we briefly present one of the GPS – INS integration approaches, along with its formulation and simulated results. In our study, we consider the open-loop tightly coupled integration architecture. The basic formulation and simulation setup is adopted from [6] and modified for our study [7].

GPS receivers require signals from at least four satellites to determine position and velocity. However, since the tightly-coupled approach uses raw GPS measurements, the algorithm can be used to aid INS even when a complete position fix is not available, i.e., when less than four satellites are visible. Hence, this approach is both robust (since it doesn't always require a complete position solution) as well as easy to implement (since only one EKF is used). In the following presentation, due to the paucity of space, we mention just the salient features of the algorithm. For basics of the EKF algorithm refer [3, 9].

A. INS Measurement Error Characteristics

As mentioned earlier, measurements from the INS are erroneous. The random errors are modeled as white noise, and the biases are often time-varying, and can be modeled as an exponentially auto-correlated process. Additionally, these sensor measurements include scale factor and misalignment errors. For ease of analysis, measurement errors are modeled as an additive sensor bias and white noise. The sensor biases are assumed to be constant (0.01 g for accelerometers and 0.1 deg/hr for gyros along each axis), and no misalignments are considered. The PSDs of the white noise in accelerometer and gyro measurements are taken same as that of Sec. II. A strapdown INS is considered, hence both acceleration and body inertial rate vector measurements are provided in the Body frame of reference. Further, the INS measurements are available at 100 Hz.

B. GPS Measurement Error Characteristics

The GPS constellation is simulated to determine the visible satellites and true pseudoranges at a given time instant. The GPS receiver measurements, in practice, include error terms from sources such as the ionosphere, troposphere, receiver and satellite clock, satellite ephemeris, multipath, and electronic noise. Some of these errors are stochastic, while some depend on time of the day, position of the receiver, and environmental conditions [8]. The pseudorange measurement (ρ) from the i^{th} GPS satellite depends on satellite position (X^i,Y^i,Z^i), receiver position (X_0,Y_0,Z_0), receiver clock bias (Δt_b), speed of light (c), and measurement noise (w^i), as described in Eq. (1).

$$\rho = \sqrt{(X^i - X_0)^2 + (Y^i - Y_0)^2 + (Z^i - Z_0)^2} + c\Delta t_b + w^i \qquad (1)$$

$$w^i_{k+1} = \lambda w^i_k + w^i_{v,k} \qquad (2)$$

In this section, a simplified model considering the GPS pseudorange measurement errors as an exponentially auto-correlated process is used for simulation (Eq. 2). (This is improved upon, and a more realistic model which explicitly considers error terms due to troposphere and ionosphere is used in the following section while utilizing the carrier phase.) The strength of the measurement error depends on the correlation parameter (λ) and standard deviation of the discrete white noise (driving the exponentially auto-correlated process) $w_{v,k}$, which are taken as 0.9983 and 0.0306 m, respectively. The error strength of the exponentially auto-correlated process is chosen so as to account for tropospheric errors, ionospheric errors and electronic noise, as would be encountered in a single-frequency receiver.

The GPS receiver clock noise, which is also a primary source of error, is modeled using a two-state model involving clock drift (d) and bias ($b = \Delta t_b$) (Eq. 3a-3b). The PSDs of the white noise v_b and v_d, are taken as, 4×10^{-20} Hz^{-1} and 8×10^{-19} $(1/s)^2/Hz$, respectively. The GPS measurements are assumed to be available at 1 Hz. For more details of GPS model considered here, see [9].

$$\dot{b} = d + v_b \tag{3a}$$

$$\dot{d} = v_d \tag{3b}$$

C. GPS-INS Integration Algorithm

The GPS-INS integration algorithm utilizes an extended Kalman filter to combine the measurements from the INS and the GPS, and provide navigation estimates. The algorithm is used to estimate 11 states which include – the position, velocity and attitude of the vehicle, and GPS receiver clock bias and clock drift. The EKF instead of estimating the total state estimates the error state, which is then used to obtain the estimate of the total state. The state vector for the EKF is given in Eq. (4), where $\boldsymbol{\delta x}$, $\boldsymbol{\delta v}$ and $\boldsymbol{\psi}$, denote position, velocity and tilt (attitude) error of the vehicle in the local vertical local horizontal (LVLH) frame.

$$\mathbf{x}_{EKF} = \begin{bmatrix} \delta\mathbf{x} & \delta\mathbf{v} & \psi & c\Delta t_b & c*d \end{bmatrix} \tag{4}$$

The INS processes the measurements of gyros and accelerometers, and through integration in the LVLH frame (also referred to as the navigation frame, with subscript n) provides an estimate of position, velocity and attitude. The mechanization equation for estimating velocity and attitude are given in Eq. (5a-5b).

$$\dot{\mathbf{v}}_n = C_{nb}\mathbf{f}_b - \left(\Omega^n_{e/n} + 2\Omega^n_{i/e}\right)\mathbf{v}_n + \mathbf{g}_n \tag{5a}$$

$$\dot{C}_{nb} = -\Omega^n_{b/n} C_{nb} \tag{5b}$$

The transformation matrix from body to navigation frame is denoted by the C_{nb} matrix, and $\Omega^z_{y/x}$ denotes the skew-symmetric cross-product matrix associated with the angular rate vector of coordinate frame x with respect to coordinate frame y expressed in the z frame. The vector $\mathbf{g_n}$ denotes the gravity vector in the navigation frame, and acceleration measurements are denoted by $\mathbf{f_b}$. The subscripts i, e, and b, denote the Earth Centered Inertial (ECI), Earth Centered Earth Fixed (ECEF), and body fixed frame, respectively.

Position of the vehicle is obtained through integration of its velocity. These estimates of position, velocity and attitude, which are available at 100 Hz due to the frequent INS measurements, are used as the process model for the aircraft and are thus used for the prediction step of the extended Kalman filter. Note that though INS provides sensor measurements, it is in fact the process model (and not the measurement model) of the EKF. However, the estimates from INS deteriorate with time due to the bias and noise in the gyro and accelerometer measurements.

On the other hand, GPS pseudorange measurements, which are available at only 1 Hz but whose errors are limited in magnitude, are used during the correction step of the EKF. Thus, GPS model represents the measurement model of the EKF. As observed in Eq. (1), the measurement model which relates pseudorange (ρ) to position is nonlinear due to the relation of pseudorange with elements of the state vector (namely position). Hence, there is a need to use the EKF for nonlinear systems. Since, an error state formulation is being used the difference between measured and estimated pseudorange is used as the effective measurement. The measurement sensitivity matrix (H) is obtained by calculating the Jacobian of the pseudorange at the predicted estimates. A single row of the sensitivity matrix for the i^{th} satellite measurement is given by Eq. (6), where the vector $\mathbf{e}_n$ denotes the line-of-sight unit vector from the receiver to the satellite. As Eq. (1) suggests, the receiver clock bias also affects the pseudorange measurement.

$$H^i = \begin{bmatrix} \mathbf{e}^i_n & 0_{3\times1} & 0_{3\times1} & 1 & 0 \end{bmatrix} \tag{6}$$

Here, even though only pseudorange measurements are considered, the filter can be adapted to utilize range rate and/or carrier phase measurements. For implementing EKF matrix parameters for quantifying uncertainty in models and the initial estimates are also required. The process noise matrix (Q) depends on the error characteristics of the accelerometers and gyros and can be obtained from either the specification sheets or ground based tests. The measurement noise matrix (R) signifies the uncertainty in GPS measurements, and is specified based on the characteristics of the GPS receiver. The initial covariance matrix (P_0), representing the current formulation depends on the knowledge of the initial state. The filter is initialized using the *a priori* estimate of state vector, which may be obtained with some additional sensors. For the simulation results presented next the matrix Q is obtained from PSD of gyro and accelerometer specified in Sec. III - A, the R matrix is taken as a diagonal matrix with each diagonal element equal to $(30m)^2$. For detailed equations and EKF parameters such as the process noise matrix (Q), measurement noise matrix (R) and initial covariance matrix (P_0), representing the current formulation refer [6-7].

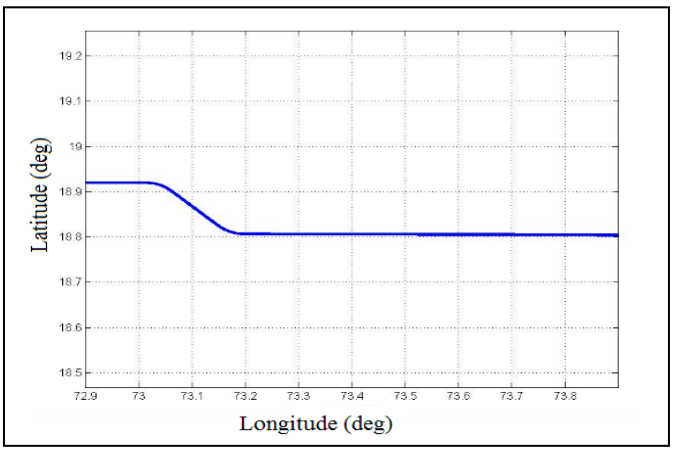

Figure 2. True Trajectory

D. Simulation Results

In order to observe the simulated performance, a true trajectory representing the real aircraft motion is required. One such trajectory for a typical simulation is presented in Fig. 2. The aircraft motion is simulated using navigation equation in the navigation frame. The aircraft initiates with a speed of 650 km/h in the east direction. The aircraft motion is governed by the bank command, and the aircraft is following the bank-to-turn maneuver, which involves a pulsed bank command resulting in change in aircraft's latitude. The position errors are represented in the ECEF frame in the plots. The position, velocity, and attitude estimation error for a simulation run are presented in Fig. 3, 4, and 5, respectively. The position accuracy though improves with the help of GPS aiding is still at the decimeter level. The envelopes in the plots represent the standard deviation of the estimation error.

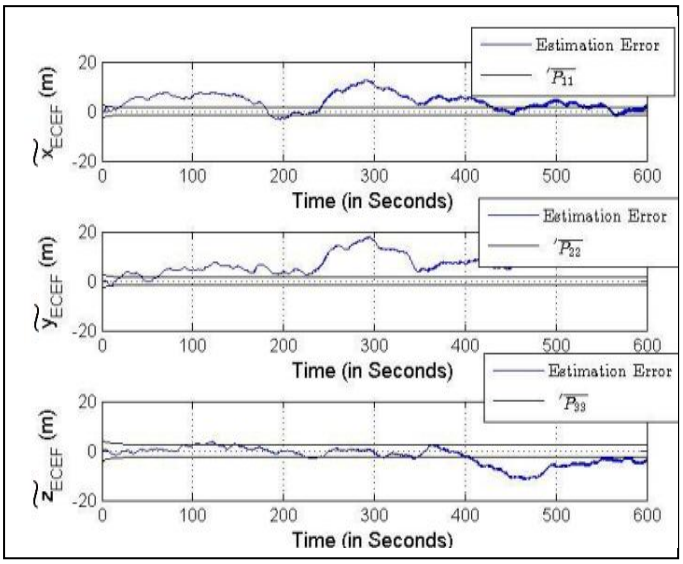

Figure 3. Estimation error in Position

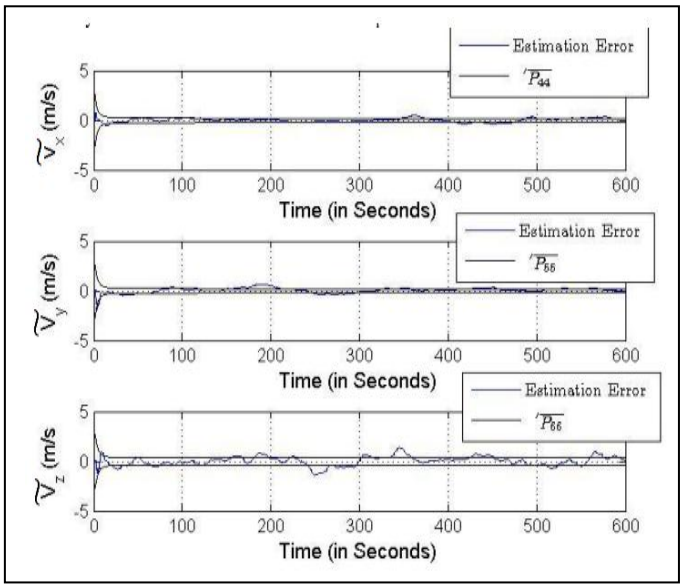

Figure 4. Estimation error in Velocity

The errors in velocity and attitude remain within the predicted bounds, as opposed to the position estimates. Similar results were obtained for a flight which incorporated a circular trajectory [7]. Note that in these simulations the aircraft is assumed to maintain the flight path, and no effect of estimation errors on aircraft control is considered. Further, simulations for larger flight time periods have been carried out in Ref. 10, which also yield decimeter level accuracy in position estimation.

Fig. 6 shows filter performance, when fewer than four GPS satellites are visible. As expected, errors increase when fewer satellites are visible; however, even with single satellite of 20 m is observed after 400 s. Hence, even in the undesirable situation of reduced visibility the filter could provide satisfactory performance for a short period of time. Using more evolved architectures the performance during such situations can be further enhanced.

E. Bias Estimation

The EKF algorithm also offers a straight-forward approach to include additional states if required; for instance, to estimate additional sensor errors. Estimation of gyro and accelerometers biases, which vary with time, can be done using the EKF framework by augmenting the process model. This may be essential for systems involving low-grade MEMS sensors. Performance of one such formulation can be observed in [10], which estimates the gyro and accelerometer biases to obtain improved estimation accuracies.

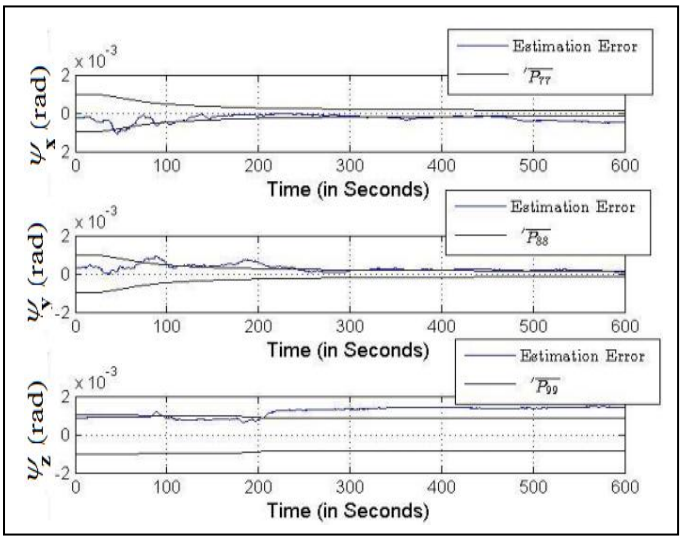

Figure 5. Estimation error in Attitude

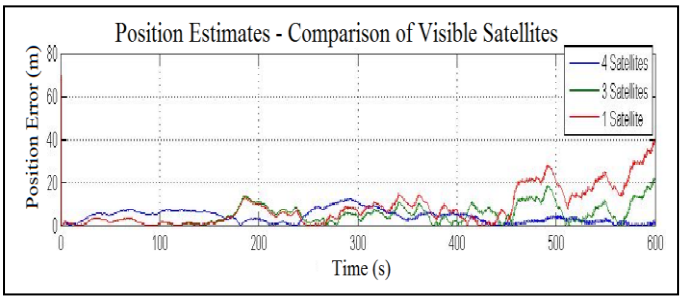

Figure 6. Position Estimates – with reduced Satellite visibility

F. Comments

The above GPS-INS integration architecture is observed to be functional and robust for position, velocity and attitude estimation. However, the decimeter-level estimation accuracy achieved for navigation, which may be sufficient for level flight operation, is inadequate for critical phases of aircraft operation, such as, Category-III autonomous landing. A standard single-frequency GPS receiver provides a positioning accuracy of around 4-20m, limiting the achievable navigational accuracy. Hence, next, we briefly analyze methods to utilize more precise GPS measurements that are available via D-GPS and single- or dual-frequency carrier phase measurements to improve the estimation performance.

V. Carrier Phase Tracking

Better processing of GPS measurements, through better hardware, and prior to using them in the GPS-INS integration algorithm, can result in substantial improvements in navigation performance. Firstly, use of a dual-frequency receiver offers a method of estimating and partially eliminating the errors due to ionosphere, a major source of measurement error in GPS [3]. This improvement may also be achieved using D-GPS through single frequency receivers, albeit with the need of a reference GPS receiver or integrity beacons. Secondly, more important is the use of carrier phase tracking approach which allows range determination with sub-centimetre level accuracy [8]. However, carrier phase tracking requires an additional estimate of unknown but fixed integer ambiguities before the receiver can begin to determine the position. The estimation of integer ambiguity is a challenging problem, and only through its accurate estimation a precise navigation solution can be achieved.

The approach presented here for carrier phase tracking requires a reference receiver. The single-difference phase measurement, utilizing user and reference measurements, depends on the geometric range between satellite and the user, and the integer ambiguity. For short baselines, i.e., when the user and reference are close the ionospheric and tropospheric errors are largely eliminated. Hence, by knowledge of the integer ambiguity precise positioning can be achieved. For a detailed mathematical formulation of the approach presented in this section, refer [11].

A. Integer Ambiguity Resolution

In order to resolve the integer ambiguity ($N_{u\text{-}r}$) for precise positioning, single-difference code phase measurements ($\rho_{u\text{-}r}$) are first calculated similar to the single-frequency carrier phase measurements ($\varphi_{u\text{-}r}$). Assuming short baselines, the smoothed pseudorange equations is obtained as shown in Eq. (7) [12].

$$\varphi_{u\text{-}r} - \rho_{u\text{-}r} \approx \lambda N_{u\text{-}r} + \varepsilon \tag{7}$$

The symbol λ denotes the GPS carrier signal wavelength and ε represents the measurement noise post the two differencing operations. A least square error estimate of the integer ambiguity can be obtained based on Eq. (7), resulting in the following simple expression (Eq. 8),

$$N_{u\text{-}r,estimate} \approx \text{round}[\lambda^{-1}(\varphi_{u\text{-}r} - \rho_{u\text{-}r})] \tag{8}$$

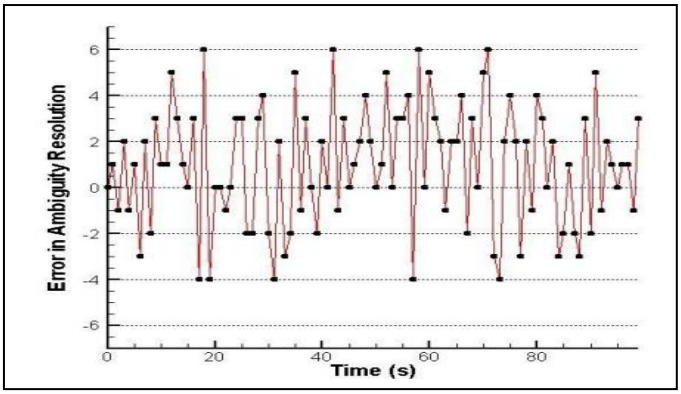

Figure 7. Integer Ambiguity Resolution [11]

which can be used at a single epoch requiring minimal computation as compared to the conventional algorithms such as the 'search methods' and the motion-based algorithms. However, these measurements are noisy, therefore to eliminate the measurement noise, the values of the integer ambiguities over multiple epochs are averaged to obtain the final estimate. Fig. 7 shows the simulation results of integer ambiguity estimation with 100 epochs. The standard deviation of error in integer estimation with 100 epochs is 2.63 cycles. Accuracy increases with the number of sample points, but this slows the process of carrier phase tracking as the aircraft must wait longer before it can switch to the precise positioning mode.

B. Simulation Results

A simplified simulation of aircraft landing which assumes an ideal INS using the approach described above is presented. Note that, in the section, the GPS solution is obtained via least square estimation instead of an EKF. In real systems, the improved GPS solution obtained using carrier phase is used as an input for the GPS-INS integration algorithm. One reference receiver, whose position is known accurately, and two integrity beacons, which are located at a distance of around 16 km on either side of the runway, are considered to broadcast their measurements and are included in the simulation. These signals from the integrity beacons and the receiver are received by GPS receiver as additional measurements and make the navigation solution more accurate as well as robust.

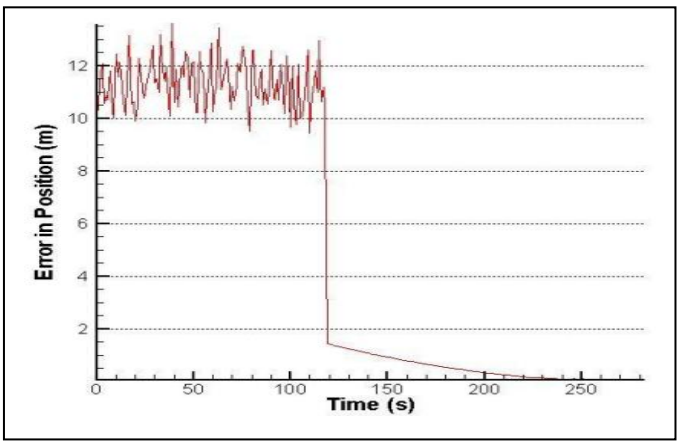

Figure 8. Position estimates – Effect of Integer Ambiguity Resolution [11]

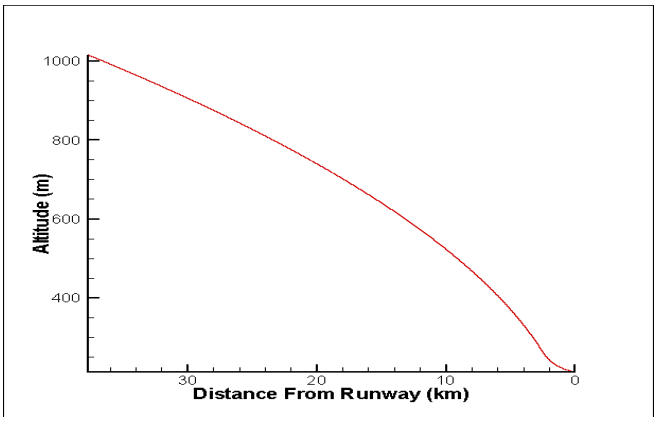

Figure 9. Aircraft Landing Trajectory [11]

A more detailed GPS model is used for the simulation presented in this section. Error in GPS measurements from terms due to the ionosphere [13] and the troposphere [14] are explicitly included instead of using the simplifying assumption of exponentially auto-correlated process. Additionally, white noise is added to the GPS measurements to model the effect of error sources apart from the ionosphere and the troposphere.

Fig. 8 shows the error in position estimates of a simulated aircraft trajectory while landing. For the initial 120 s, the aircraft is collecting carrier phase measurements but relies only on code measurements as the integer ambiguity is unknown. Through these collected measurements integer ambiguity is estimated using Eq. (8), and is used to correct the phase measurements after 120 s. The corrected carrier phase measurements result in a steep error reduction in position estimates from around 10 m to 1.5 m. As time progresses, the error is seen to gradually reduce to sub-cm level accuracy.

Closed loop simulations for automatic aircraft landing which include effect of aircraft navigation as well as control are also carried out. A parabolic continuous descent trajectory and aircraft parameters of Boeing 747 are used for simulating the aircraft trajectory. Fig. 9 shows the true trajectory highlighting the parabolic continuous descent approach. Fig. 10 shows the vertical deviation from the commanded glide slope achieved by the closed loop system. The sub-meter level errors observed in Fig. 10 are due to the effects of aircraft control and

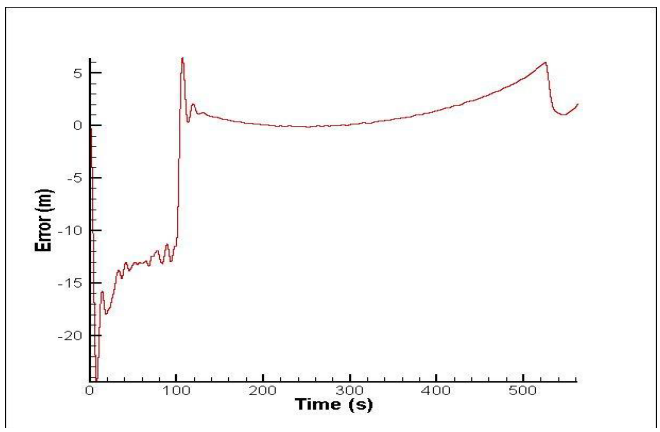

Figure 10. Vertical Deviation from Glideslope [11]

are much larger than the navigation accuracy, indicating the need for detailed closed loop analysis. For detailed results of aircraft landing, see [11].

VI. Conclusion

In this paper, through analysis and simulation of an open-loop tightly coupled GPS-INS integration architecture which utilizes raw pseudorange measurements, satisfactory navigation accuracy has been obtained for level flight. The filter is observed to be robust, as it functions even when fewer than 4 GPS satellites were visible. However, for critical phases such as aircraft landing, carrier phase tracking is essential to achieve desired estimation performance. A technique for integer ambiguity resolution has been presented to utilize GPS carrier phase measurements. Basic simulation results of navigation during aircraft landing using carrier phase measurements show remarkable improvements in estimation accuracy. Future work would include investigation of the above approaches through more detailed closed-loop simulation. Detailed model of aircraft dynamics, controls and sensor (GPS and INS) errors would be incorporated to make the simulation more realistic. Further, improvements in algorithm for considering sensor misalignment, and GPS redundancies will also be considered.

References

[1] D. H. Titterton and J. L. Weston, Strapdown Inertial Navigation Technology, 2nd ed., AIAA, 2004.

[2] B. W. Parkinson, ed. Global Positioning System: Theory and Applications, 1st ed., vol. 1. Progress in Aeronautics and Astronautics series, AIAA, 1996.

[3] M. S. Grewal, L. R. Weill, and A. P. Andrews, Global Positioning Systems, Inertial Navigation, and Integration, 2nd ed., Wiley, 2007.

[4] P. D. Groves, Principles of GNSS, Inertial, and Multisensor Integrated Navigation Systems, 1st ed., Artech House, 2008.

[5] A. Sharma, "GAGAN: GPS Aided Geo Augmented Navigation," *B.Tech Thesis*, Indian Institute of Technology Kanpur, Mar, 2009.

[6] R. M. Rogers, Applied Mathematics in Integrated Navigation Systems, 3rd ed., AIAA Education Series, 2007, pp. 229-245.

[7] V. V. Unhelkar, "GPS-Aided INS with Applications to Aircraft Turns," *B.Tech Thesis*, Indian Institute of Technology Bombay, May, 2011.

[8] P. Misra and P. Enge, GPS Signals, Measurements, and Performance, 2nd ed., Ganga-Jamuna Press, 2006, pp. 233-280.

[9] Y. Bar-Shalom, X. Li, and T. Kirubarajan, Estimation with Applications to Tracking and Navigation, John Wiley & Sons, 2001, pp. 491-515.

[10] A. Sharma, P. Kumar, S. M. Ratnaker, and S. E. Talole, "Accurate navigation of a UAV using Kalman filter based GPS-INS integration," Paper No. 208, *in Proceedings* of the 5th Symposium on Applied Aerodynamics and Design of Aerospace Vehicles, Bangalore, 2011.

[11] S. Agarwal and H. B. Hablani, "Automatic Aircraft Landing over Parabolic Trajectory using Precise GPS Measurements," IJCA Proceedings on International Conference and workshop on Emerging Trends in Technology (ICWET), (7):38-45, 2011.

[12] J.B. Lundberg and S.P. Yoon, "An Integer Ambiguity Resolution Algorithm for Real Time GPS Attitude Determination," Applied Mathematics and Computation, Elsevier, vol. 129, pp. 21-41, 2002.

[13] Klobuchar, J.A., A First-Order, Worldwide, Ionospheric Time Delay Algorithm, AFCRL-TR-75-0502, AD A018862, available from the Defense Technical Information Center, Cameron Station, Alexandria, VA 22304.

[14] Hopsfield, H.S., Tropospheric Effect on Electromagnetically Measured Range: Prediction from Surface Weather Data, Applied Physics Laboratory, Johns Hopkins University, Baltimore, MD, July 1970.